A fundamental study of the reductive leaching of chalcopyrite using metallic iron part I: kinetic analysis

David Dreisinger [*], Nedam Abed

Department of Metals and Materials Engineering, University of British Columbia, 309-6350 Stores Road, Vancouver, BC, Canada V6T 1Z4

Abstract

The reductive leaching (decomposition) of chalcopyrite was studied in an attempt to find a suitable hydrometallurgical method for copper recovery. A chalcopyrite concentrate was leached under reducing conditions, where metallic iron served as a reductant. The studied parameters include agitation, temperature, particle size, acidity, and reductant and chalcopyrite amounts. The experimental results showed that it is possible to convert the refractory chalcopyrite to a rich copper sulfide (chalcocite), which is amenable to further treatment. The results of kinetic analysis of the leaching data under various experimental conditions indicated a reaction controlled by the solution transport of protons through the product layer, with an activation energy of 33.9 kJ/mol for sulfate media and 22.4 kJ/mol for chloride media. Based on the shrinking core model, the following rate equation was established for sulfate media:

$$1 - 3(1 - X_b)^{2/3} + 2(1 - X_b) = \frac{k_o'}{R^2}[H^+]\exp\left(\frac{-33,880}{R'T}\right)t$$

and for chloride media,

$$1 - 3(1 - X_b)^{2/3} + 2(1 - X_b) = \frac{k_o''}{R^2}[H^+]\exp\left(\frac{-22,423}{R'T}\right)t$$

The results of the kinetic analysis were utilized in developing a simple process for producing copper super-concentrates. The process still needs further investigation to demonstrate its viability.
© 2002 Elsevier Science B.V. All rights reserved.

Keywords: Reductive leaching; Chalcopyrite; Metallic iron

1. Introduction

The hydrometallurgical treatment of copper sulfide concentrates is increasingly establishing itself as a viable route for the extraction of copper and recovery of associated precious metal values. This is attributed to the merits of this route that include suitability for low-grade and complex ores, high recoveries, competitive economics, and other operational features.

A quick review of proposed hydrometallurgical treatment methods for chalcopyrite and other copper sulfides (Prasad and Pandey, 1998; King and Dreisinger, 1995; Venkatachalam, 1991; Peters et al., 1981; Dutrizac and MacDonald, 1974; Dasher,

* Corresponding author. Fax: +1-604-822-3619.

1973; Paynter, 1973; Roman and Benner, 1973; Subramanian and Jennings, 1972) shows that they are generally either in sulfate or chloride media. Processes in sulfate media include acid pressure leaching, ferric sulfate leaching, bacterial leaching, and others. Processes in chloride media include ferric chloride leaching, cupric chloride leaching, chlorine and hydrochloric acid leaching, and others. Cyanide, ammoniacal, and nitric acid leaching processes are also reported in the open literature.

Although hydrometallurgy is put forward as a preferred alternative to pyrometallurgy, on the basis of economics and environmental protection, many of the proposed hydrometallurgical methods have the following features: codissolution of copper and iron, extreme conditions of temperature and pressure or very fine grinding of concentrates are required, quan-

titative yield of elemental sulfur is not achieved, precious metal recovery is difficult and several complex unit operations are needed for a complete flowsheet. These facts explain why hydrometallurgical routes for copper sulfide concentrate treatment have found little commercialization.

Virtually all of the copper hydrometallurgical processes under current development use oxidative decomposition of chalcopyrite as the primary method of treatment. An alternate approach to treatment of chalcopyrite would be to perform a reductive decomposition step. This reductive decomposition would in effect transform the chalcopyrite to a much more reactive form (e.g. chalcocite), perhaps allowing further hydrometallurgical treatment of the reduced concentrate. The reductive method allows for the rejection of iron and some sulfur, where a rich copper
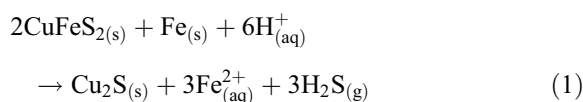
Table 1
Summary of published research on reductive leaching of chalcopyrite

Researcher(s)	Reductant	Remarks
Hiskey and Wadsworth (1975)	copper in H_2SO_4 solution	• chemical control with activation energy (E_a) of 48.12 kJ/mol • galvanic mechanism • rate is dependent on hydrogen ion concentration $[H^+]$ • rate is independent of initial particle size of chalcopyrite • agitation is detrimental to conversion • Cu^{2+} is detrimental to conversion while Fe^{2+} is not • products: Cu_2S with some Cu_5FeS_4 and $Cu_{1.95}S$
Sohn and Wadsworth (1980)	SO_2 with $CuSO_4$	• chemical control with E_a of 77.5 kJ/mol • corrosion mechanism • agitation is required • rate is dependent on initial particle size of chalcopyrite • rate is dependent on Cu^{2+} concentration • Fe^{2+} has a catalytic effect • product: $Cu_{1.95}S$ followed by Cu_5FeS_4
Hackl et al. (1987)	H_2 with $CuSO_4$	• H_2 reduction of Cu^{2+} followed by Cu reduction of $CuFeS_2$ • galvanic mechanism • complete dissolution of chalcopyrite iron component • Cu_2S is the product
Hackl et al. (1987)	copper under autoclave conditions	• controlled by the outward transport of Fe^{2+}, $E_a = 67$ kJ/mol • galvanic and Cu^+-mediated mechanisms • 97% dissolution of chalcopyrite iron component • Cu_2S is the product
Chae and Wadsworth (1979)	lead in HCl solution	• controlled by transport of electrons with E_a of 28.1 kJ/mol • combined corrosion-galvanic mechanisms • rate is independent of chalcopyrite and lead particle sizes • products: $Cu_{1.95}S$ followed by Cu
Shirts et al. (1974)	iron in H_2SO_4 and HCl solutions	• controlled by a transport process • two stages of leaching • rate is dependent on acid concentration and reductant amount • twice the stoichiometric amount of reductant is required • Cu_2S is the product

sulfide (chalcocite) is formed, using a suitable reductant, such as metallic iron. Iron as a reductant has some advantages, including low price, good availability, and full compatibility with the leach solution.

Reductive leaching is reported to be an electrochemical process composed of an anodic portion, which is the reductant dissolution, and a cathodic portion which is chalcopyrite reduction, i.e. collapse of its crystal structure. The thermodynamic description of chalcopyrite leaching can be found in Peters (1976). Also, several studies on reductive leaching have been published as summarized in Table 1.

Unfortunately, none of these studies resulted in commercial development. Where iron was used as the reductant, published work has been qualitative in nature. It is therefore desirable to understand the physical chemistry of the leaching reaction:

$$2CuFeS_{2(s)} + Fe_{(s)} + 6H^+_{(aq)}$$
$$\rightarrow Cu_2S_{(s)} + 3Fe^{2+}_{(aq)} + 3H_2S_{(g)} \qquad (1)$$

and establish the conditions or combination of conditions that make this noncatalytic solid–fluid reaction a viable alternative, with the possibility of developing a process flowsheet.

We report here the results of such a study with emphasis on kinetic analysis, as was confirmed from chemical and microscopic analysis. Based on the results obtained, a simple process flowsheet is proposed.

2. Experimental

2.1. Materials

A chalcopyrite concentrate was obtained from Gibraltar Mine, McLeese Lake, BC, Canada. The

Table 2
Detailed chemical analysis of the tested chalcopyrite concentrate

Element	Mass (%)
Copper	28.3
Iron	28.0
Sulfur (%)$_{total}$	30.0
Sulfur, S^{2-} (%)	32.0
Molybdenum	0.4
Insoluble (%)[a]	10.7

[a] As siliceous gangue.

Table 3
The mineralogical composition of the tested chalcopyrite concentrate

Mineral	Content (mass %)
Chalcopyrite (CuFeS$_2$)	63.8
Pyrite (FeS$_2$)	17.0
Chalcanthite (CuSO$_4$·5H$_2$O)	9.3
Siliceous gangue and other refractory oxides	9.9

detailed chemical analysis of the concentrate (ICP method) is given in Table 2. The mineralogical composition is provided in Table 3; this composition was obtained using X-ray diffraction (XRD) and verified by the Rietveld method (O'Connor et al., 1992).

The concentrate samples were prepared as follows: the bulk ore was first split by coning and quartering techniques, then a sample weighing around 35 kg was split again using a riffle to obtain a representative sample for the kinetic study. The obtained sample, around 2 kg, was first wet screened to remove extremely fine particles which could bias initial leaching data, followed by rinsing with acetone and/or ethanol to allow fast drying. The remaining sample was then subjected to a careful dry screening into discrete size fractions (monosizing). Desired size fractions were separated and kept under inert atmosphere to be used in the experiments. Unless otherwise specified, particle size used was −100/+200 mesh (−149/+74 μm).

All the chemical reagents were of analytical grade and were used as received. Analytical grade metallic iron used in the experiments was in powdery form (−600 mesh) and produced by electrolytic reduction. Deionized water was used in the experiments, which were performed under atmospheric pressure.

2.2. Methods

Most of the experiments were done batchwise. The estimated amounts of concentrate and reductant were added to a solution at the required acidity level. The term "stoichiometric" refers to amounts of reactants as per Eq. (1). Reaction extent was monitored by maintaining a constant pH value, with solution sampling at regular periods. The set point of pH is the measured one by the pH probe based on the initial acid concentration.
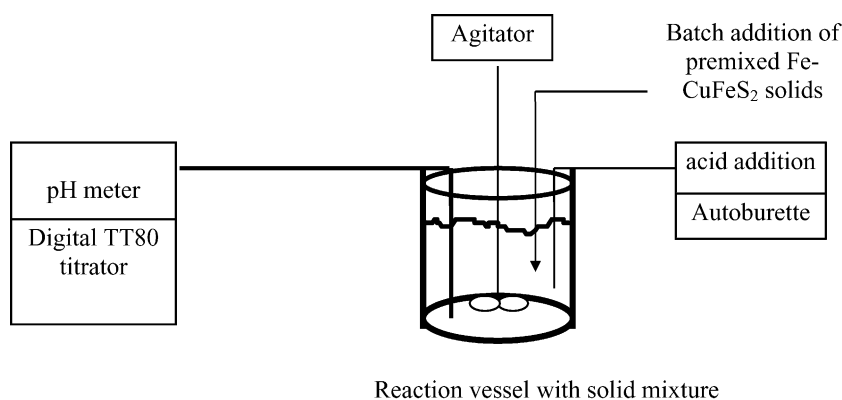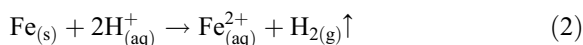
Fig. 1. Schematic diagram of the reaction vessel during the kinetic study.

Chemical analysis for iron and copper in the leach solution was done using atomic absorption spectroscopy (AAS). Leach residue was digested with bromine-water/aqua-regia mixture and the digestion solution was analyzed for copper and iron. Fig. 1 shows the experimental set-up for the kinetic study.

With regard to Eq. (1), the extent of reaction is estimated depending on the amount of iron released from chalcopyrite, through analysis of dissolved iron in solution. Under reducing conditions, only the iron component of chalcopyrite dissolves. However, because iron is the reductant, it is susceptible to dissolution in acidic media according to the following reaction:

$$Fe_{(s)} + 2H^+_{(aq)} \rightarrow Fe^{2+}_{(aq)} + H_{2(g)}\uparrow \qquad (2)$$

That is, there are two competing reactions in the system. The contribution of chalcopyrite reduction (reaction 1) and hydrogen evolution reaction (reaction 2) were separated mathematically (Abed, 1999) to follow the reduction leaching kinetics. In this context, the rates of reactions 1 and 2 were assumed to be identical. This was merely an approximation to simplify the calculations (see below). The following equation was used to provide an estimate of the extent of chalcopyrite conversion with time:

$$X_b = \frac{2 \times \Theta \times [Fe^{2+}]_{metal} \times \eta_{Fe}}{[Fe^{2+}]_{CuFeS_2}} \qquad (3)$$

Here, X_b represents the conversion of chalcopyrite or fraction of iron released from its crystal, $[Fe^{2+}]_{CuFeS_2}$ is the total iron content in chalcopyrite, $[Fe^{2+}]_{metal}$ is the concentration of iron due to complete metal dissolution, Θ is the ratio of total dissolved iron in solution at time t to that at the end of reaction and η_{Fe} is the fraction of added iron that was actually used in chalcopyrite reduction. η_{Fe} represents the overall efficiency of iron as a reductant toward chalcopyrite alone and equals the final conversion of chalcopyrite derived from chemical analysis and reaction stoichiometry.

This procedure was used to simplify the calculations because it was consistent with chemical analysis of leach residue. An alternative to this method is to estimate the amount of hydrogen sulfide generated using gas chromatography, which is beyond the scope of this research.

3. Results and discussion

3.1. Conversion-time diagrams

Figs. 2 and 3 show the extent of reaction with time. It can be seen that reaction kinetics are fast in the first hour of reaction time, but slowing or ceasing in the remaining period. This means that the first 60 min of leaching are of primary importance for kinetic analysis. The rapidness of reaction kinetics implies that leaching shown in Eq. (1), which is electrochemical in nature, might not be controlled by a chemical reaction. It can be concluded here that as soon as the solid
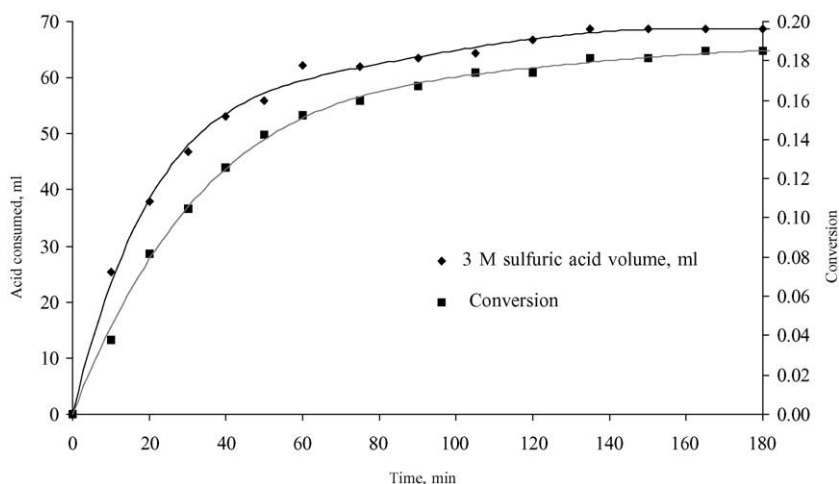
Fig. 2. Plot of acid consumption and conversion vs. time (sulfate media, stoichiometric amounts, 25 °C).

particles are contacted in the leach solution, the galvanic couple is formed and reaction products are immediately released.

3.2. Effect of agitation

Many leaching processes for fine particles require agitation to suspend solid particles and allow efficient mixing in the leach solution. Reductive leaching is an electrochemical process that depends on efficient galvanic contact between the solid particles (metal sulfide and reductant). It is therefore possible that excessive agitation may interrupt galvanic contact, and this what was found from the experiments.

Figs. 4 and 5 summarize the findings of leaching at different agitation speeds. These figures show that conversion is almost independent of agitation speed, on the basis of initial rate data, and so high-speed stirring is not required. Because of the trend of the conversion curves in Figs. 4 and 5, most of the experiments in this research were performed at an agitation speed of 250 rpm. By this selection, solid particles were kept suspended in solution, while the galvanic coupling was judged to be adequately maintained.
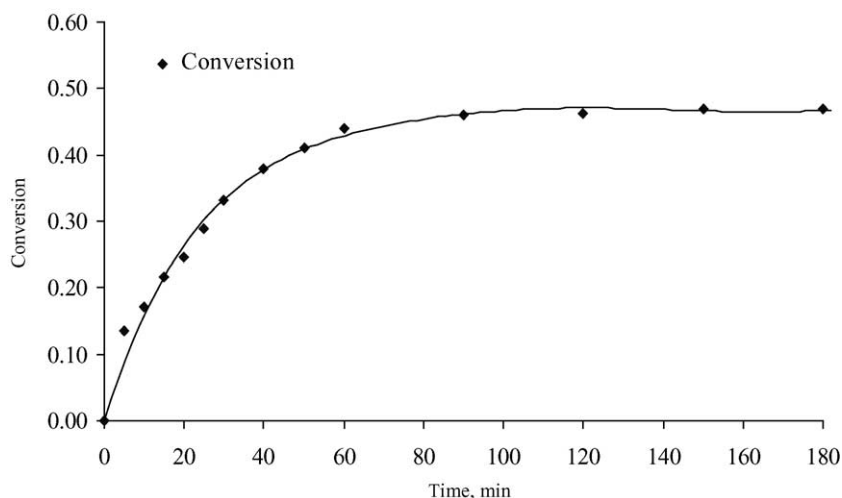

Fig. 3. Plot of conversion vs. time (chloride media, stoichiometric amounts, 65 °C).
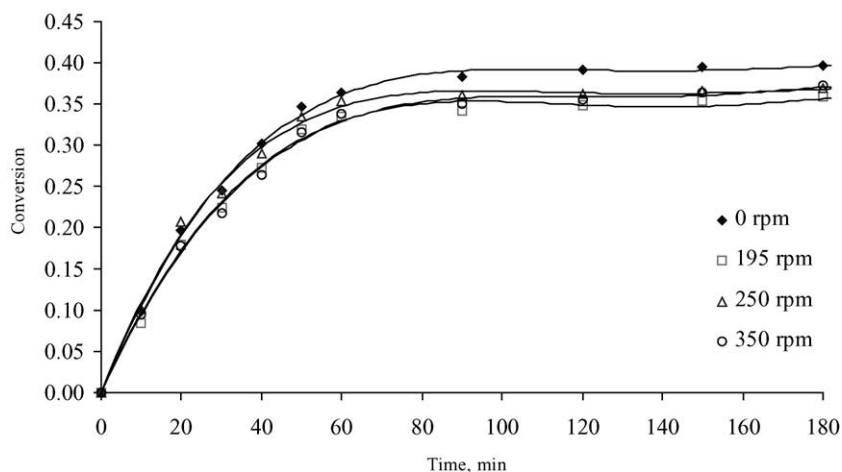
Fig. 4. Plot of conversion vs. time at various agitation speeds (sulfate media, stoichiometric amounts, 25 °C).

3.3. Temperature effect

Temperature dependence can be used to estimate the apparent activation energy, enthalpy of activation and entropy of activation. It is widely accepted (Levenspiel, 1972) that systems with an activation energy greater than 40 kJ/mol are controlled by a chemical reaction (linear leaching), while those with an activation energy less than 40 kJ/mol are controlled by a transport process (parabolic leaching), whether in the product layer or a boundary fluid film.

Experiments were performed to study the reaction temperature-dependence, which are summarized in Figs. 6 and 7. It can be seen from these figures that increasing the temperature above 65 °C is not of benefit for this leaching system. The reaction rate diminishes for temperatures greater than 65 °C. There is some improvement in reaction kinetics upon increasing the temperature to this limit, with the possibility of doubling the final conversion. This behavior of temperature dependence is common to systems controlled by a transport process. Seemingly, complete conversion is
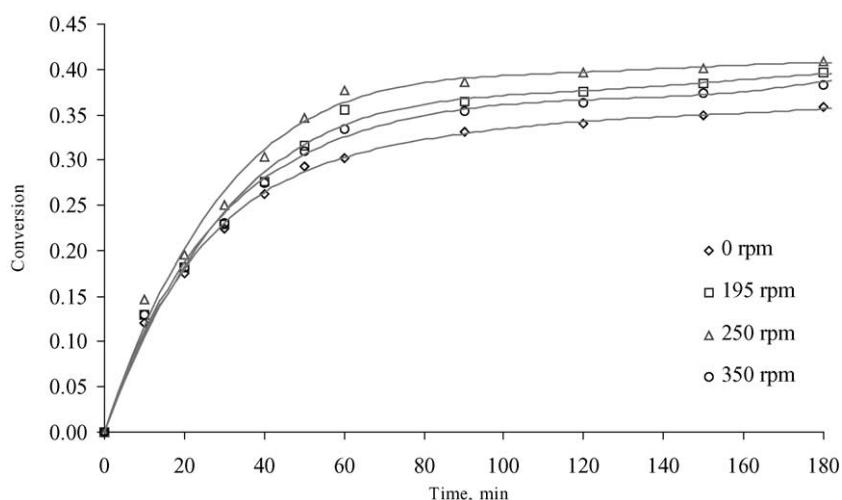

Fig. 5. Plot of conversion vs. time at various agitation speeds (chloride media, stoichiometric amounts, 25 °C).
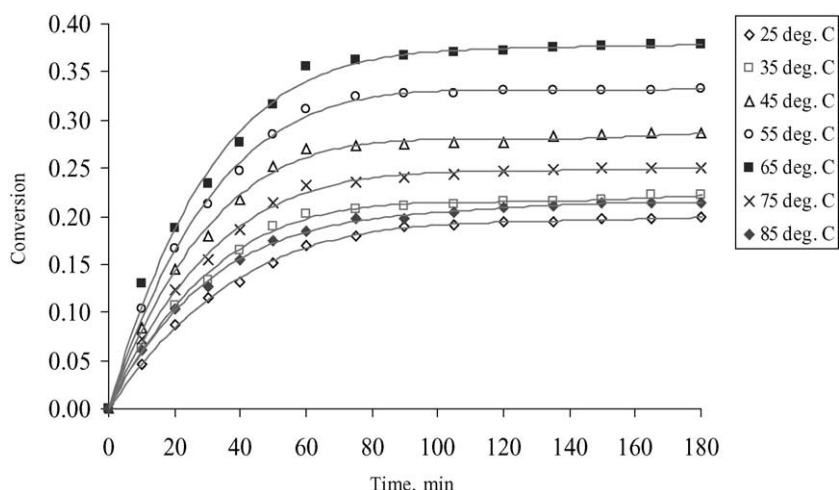
Fig. 6. Plot of conversion vs. time at various temperatures (0.1 M H_2SO_4, stoichiometric amounts).

not achieved under these conditions due to the presence of side reactions, especially the hydrogen evolution reaction (Eq. (2)). This reaction is endothermic and increasing the temperature would favor its occurrence. It is necessary, therefore, to find some method to lessen its tendency, as explained below.

For chemically controlled processes, small increments in temperature usually lead to tremendous enhancement of reaction kinetics. In the present case, the leach kinetics are only mildly affected by temperature. In addition, since leaching kinetics are not greatly affected by agitation speed (Figs. 4 and 5 and see below), it can initially be assumed that this

leaching system is controlled by a transport process in the product layer.

The kinetic equation for reactions controlled by transport through a product layer (Levenspiel, 1972) is shown below:

$$1 - 3(1 - X_b)^{2/3} + 2(1 - X_b) = kt \qquad (4)$$

where:

$$k = \frac{6bD_eC_{A_f}}{\rho_B R^2} \qquad (5)$$

and this model is only applicable to particles of unchanging size. The kinetic data from the temper-
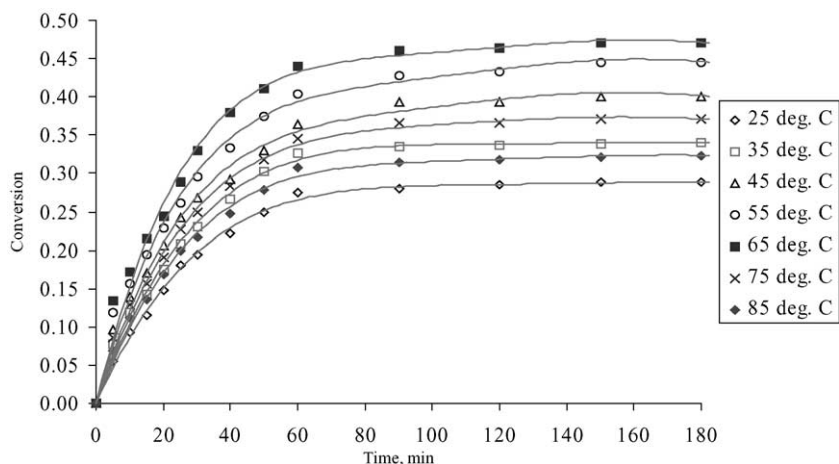

Fig. 7. Plot of conversion vs. time at various temperatures (0.1 M HCl, stoichiometric amounts).
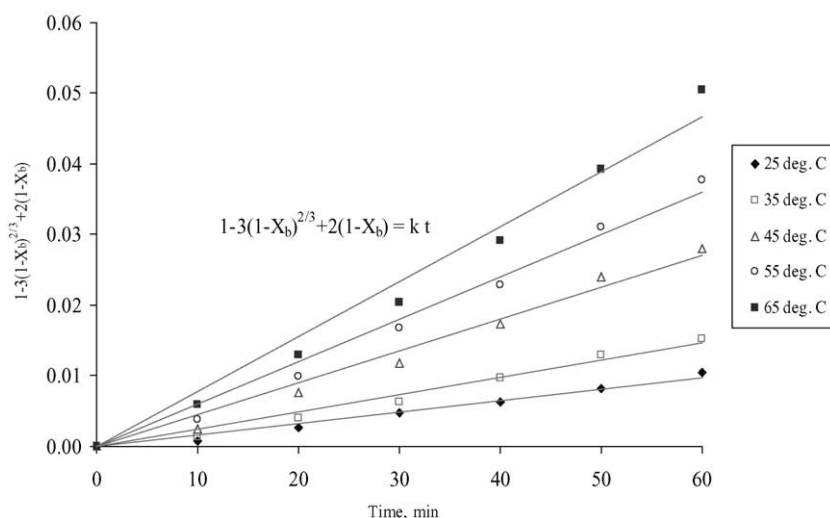
Fig. 8. Plot of product layer model fitting of conversion vs. time at various temperatures (0.1 M H_2SO_4, stoichiometric amounts), based on Fig. 6.

ature studies were fitted to Eq. (4) and the rate data were used to construct Arrhenius plots and find the apparent activation energy while the transition state theory was used to find the enthalpy and entropy of activation (Levenspiel, 1972). Figs. 8 and 9 show the conversion data fitted through Eq. (4), while Figs. 10 and 11 show the Arrhenius plots. The estimated values are summarized in Table 4.

There is a small discrepancy in the estimated value of activation energy and enthalpy of activation, which is common in most hydrometallurgical systems. It can also be attributed to experimental errors and the theoretical basis of both values. The estimated activation energy for the studied systems lies within the normal range for reactions controlled by a transport process in the product layer (Levenspiel, 1972). It confirms that the selected model is the preferred one and agrees well with the observation of mild effect upon increasing the temperature. As can be seen from Table 4, the activation energy for chloride-based
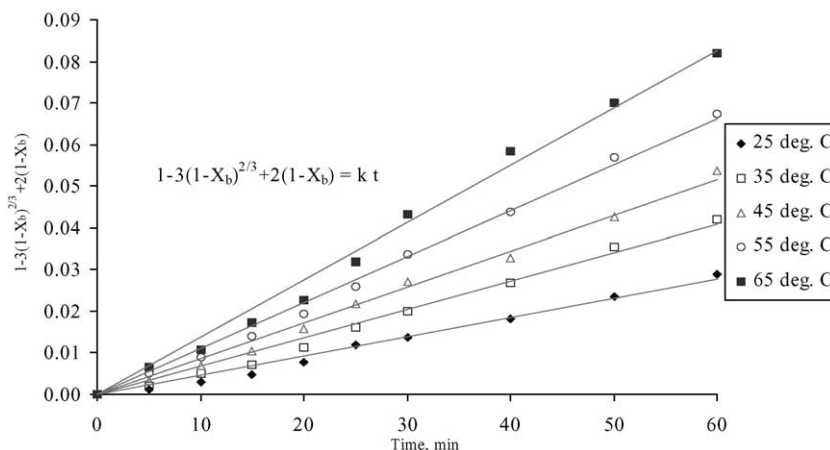

Fig. 9. Plot of product layer model fitting of conversion vs. time at various temperatures (0.1 M HCl, stoichiometric amounts), based on Fig. 7.
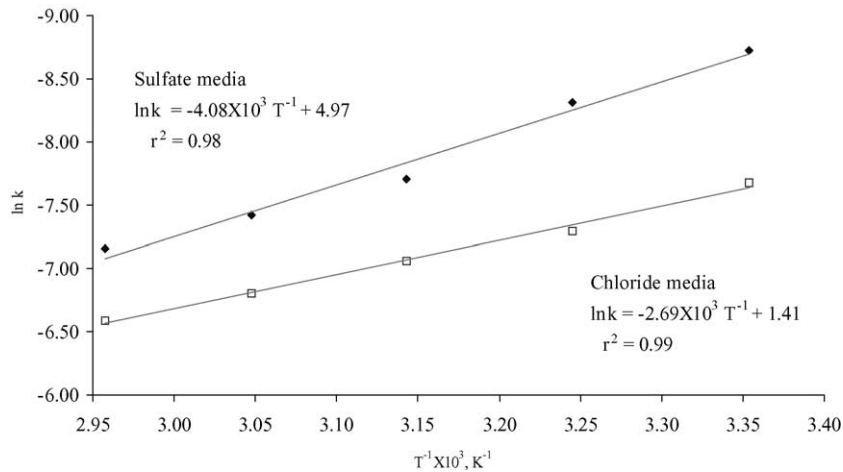
Fig. 10. Plot of reaction rates vs. inverse of temperature (Arrhenius plot) for sulfate and chloride media, based on Figs. 8 and 9.

system is smaller than that for sulfate-based system, which indicates that leaching kinetics in chloride media are less dependent on temperature compared to those in sulfate media.

The value of enthalpy or energy of activation suggests that heat had to be provided to the leaching solution (that is, by increasing the temperature) to facilitate the reactions. This is evident from the performed experiments where some improvement in reaction kinetics was obtained by increments in temperature (Table 4). The decrease in conversion beyond 65 °C is attributed to the severe competition from side reactions, such as that shown in Eq. (2).

Temperature-dependence analysis also gives another important information, which is the required time for complete leaching under different temperatures, but with the same size fraction ($-149/+74$ μm). Based on the rate constants shown in Table 4, the leaching rate or rate of particle core shrinking (the product of average particle size multiplied by the estimated rate constants), measured in micrometers per minute, can be calculated for different temperatures (Fig. 12). For example, at 65 °C and for a 50 μm chalcopyrite particle, 575 min are needed for complete conversion in sulfate media. In chloride media, the required time is 325 min, indicating that
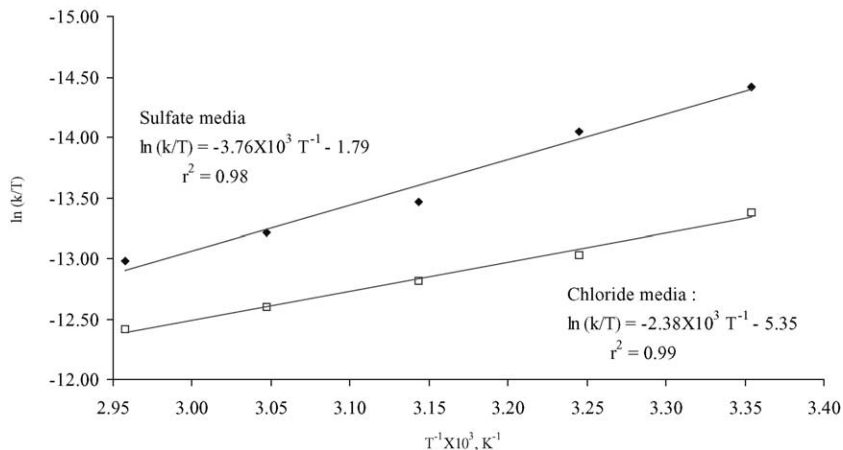

Fig. 11. Plot of ln (k/T) vs. inverse of temperature for sulfate and chloride media, based on Figs. 8 and 9.

Table 4

Temperature dependence of reaction kinetics and related thermodynamic values for sulfate and chloride media

Temperature (°C)	Parabolic leaching rate constant, k (min^{-1}) (sulfate media)	Parabolic leaching rate constant, k (min^{-1}) (chloride media)
25	1.63×10^{-4}	4.62×10^{-4}
35	2.45×10^{-4}	6.78×10^{-4}
45	4.51×10^{-4}	8.61×10^{-4}
55	6.01×10^{-4}	11.04×10^{-4}
65	7.79×10^{-4}	13.74×10^{-4}
Term	**Value (sulfate media)**	**Value (chloride media)**
Activation energy (kJ/mol)	33.9	22.4
Enthalpy of activation (kJ/mol)	31.3	19.8
Entropy of activation (J/mol per K)	-212.4	-242.0

Experimental conditions are as per Figs. 6 and 7.

leaching in chloride media is more efficient than in sulfate media. At 45 °C, the same particle requires 995 and 520 min in sulfate and chloride media, respectively, for complete conversion.

3.4. Particle size dependence

The other important factor to be studied is the effect of particle size. Determining the proper particle size range is important for economic evaluation because it is directly related to power requirement, residence time in the reaction vessel, or reactor volume, and other ore preparation methods.

Depending on the method explained earlier, discrete size fractions were prepared for leaching experiments. The smallest size fraction studied was $-44/+38$ μm and the results for sulfate and chloride media are summarized in Figs. 13 and 14, respectively. It can be seen from these figures that particle size plays an important role in the leaching process under reducing conditions. It is possible to double the final conversion of chalcopyrite by using the size fraction $-44/+38$ μm instead of $-90/+74$ μm. The kinetic data in Figs. 13 and 14 are fitted according to Eq. (4), and the results are given in Figs. 15 and 16. Table 5 summarizes the results of reaction rates dependence on
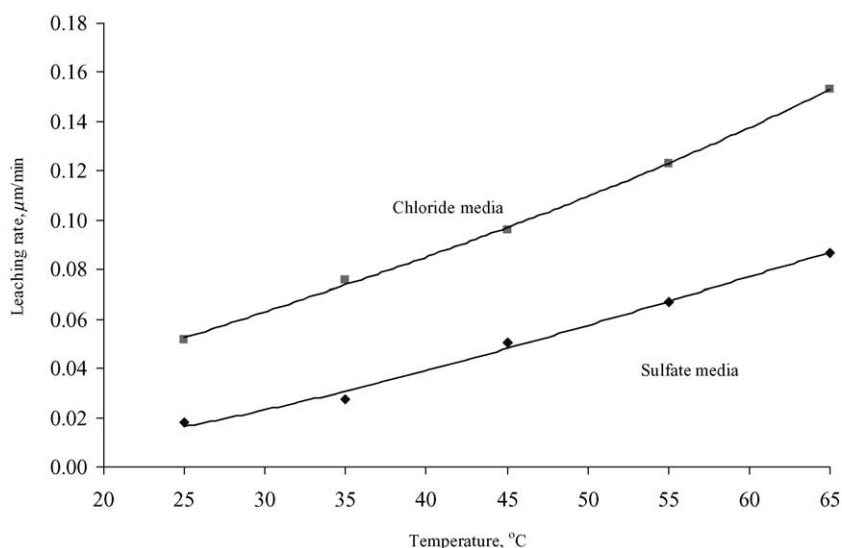

Fig. 12. Plot of chalcopyrite leaching rates vs. temperature. The experimental conditions are the same as those in Figs. 6 and 7.
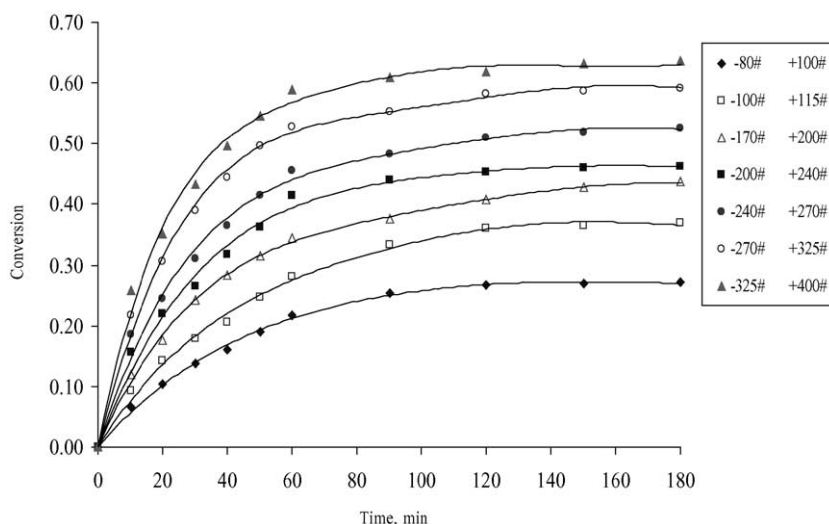
Fig. 13. Plot of conversion vs. time at various particle sizes (0.1 M H$_2$SO$_4$, stoichiometric amounts, 25 °C).

particle size. It is obvious that a 10-fold improvement in reaction rates can be obtained upon using the finest particle size instead of the coarse one.

The clear dependence on particle size is common for reactions controlled by a transport process in the product layer, which is perceived from Eq. (5). Leaching kinetics for diffusion-controlled reactions are related to the inverse square of initial particle diameter or radius, while those controlled by a chemical reaction vary with the inverse of initial particle diameter or radius. It is apparent from Eq. (5) that

small particles require much shorter time for complete conversion than do large ones. Hence, diffusion-controlled kinetics are generally improved when fine particles are used, as is the case with the current system.

Apparently, fine particles resulted in better conversion or enrichment of chalcopyrite. It can be concluded here that fine particles reduce the tendency of side reactions (Eq. (2) for example), and favor Eq. (1) to take place. Therefore, it is necessary to further investigate the effect of using even very fine particles
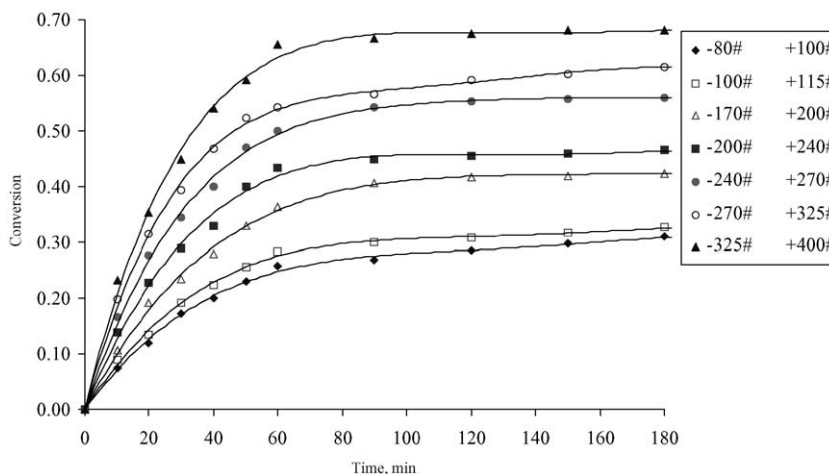

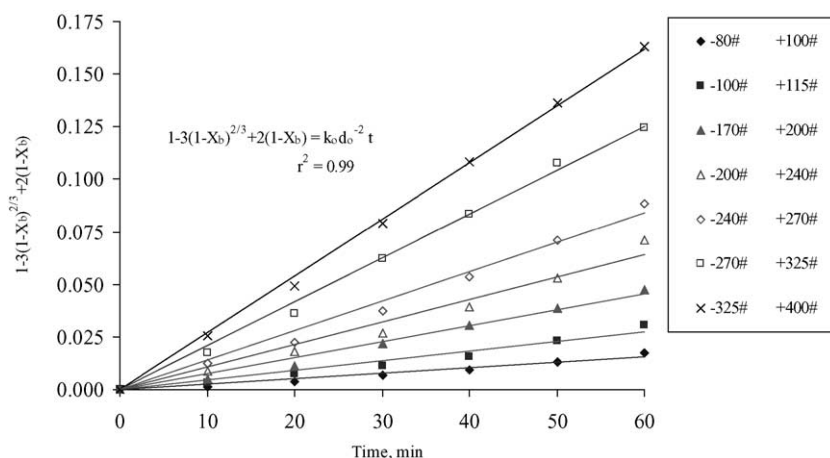Fig. 14. Plot of conversion vs. time at various particle sizes (0.1 M HCl, stoichiometric amounts, 25 °C).

Fig. 15. Plot of product layer model fitting of conversion vs. time at various particle sizes (0.1 M H$_2$SO$_4$, stoichiometric amounts, 25 °C). The data are based on Fig. 13.

(smaller than 38 μm), which is expected to make such a reductive decomposition reaction more successful.

Utilizing the definition of the parabolic leaching rate constant, k, Eq. (5) can be written as:

$$k = \frac{k_o}{R^2} \tag{6}$$

and the intrinsic parabolic leaching rate constant, k_o, now includes all the remaining constants. Eq. (6) shows that a plot of k vs. the inverse square of particle radius or diameter would yield a straight line with zero intercept for parabolic leaching kinetics. Based on the data in Figs. 13 and 14 (see also Table 5), Fig.

17 is the required plot, confirming the validity of the early assumption of product layer transport-controlled reactions.

With these findings in hand, more explanation can be given to the observed behavior at different agitation speeds. According to Levenspiel (1972), when a product layer forms, the resistance to fluid transport through this product layer is usually much greater than through the fluid film surrounding the particle. Hence, in the presence of such a product layer, fluid film resistance can safely be ignored, and product layer resistance is unaffected by changes in fluid velocity (that is, the rate of agitation in batch sys-
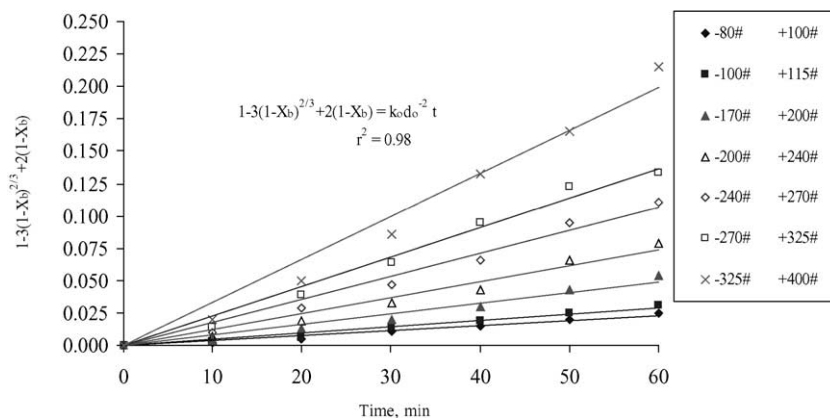

Fig. 16. Plot of product layer model fitting of conversion vs. time at various particle sizes (0.1 M HCl, stoichiometric amounts, 25 °C). The data are based on Fig. 14.

Table 5
Particle size dependence of reaction rates for sulfate and chloride media

Mesh size (#)	Particle size (μm)	Mean CuFeS$_2$ particle diameter (μm)	Parabolic leaching rate constant, k (min^{-1}) (sulfate media)	Parabolic leaching rate constant, k (min^{-1}) (chloride media)
−325/+400	−44/+38	41.0	2.695×10^{-3}	3.321×10^{-3}
−270/+325	−53/+44	48.5	2.087×10^{-3}	2.277×10^{-3}
−240/+270	−63/+53	58.0	1.396×10^{-3}	1.773×10^{-3}
−200/+240	−74/+63	68.5	1.066×10^{-3}	1.231×10^{-3}
−170/+200	−90/+74	82.0	0.761×10^{-3}	0.821×10^{-3}
−100/+115	−149/+125	137.0	0.452×10^{-3}	0.481×10^{-3}
−80/+100	−180/+149	164.5	0.261×10^{-3}	0.386×10^{-3}

Experimental conditions are as per Figs. 13 and 14.

tems). This is in conformance with the findings in this research.

3.5. Effect of initial acid concentration

It is necessary to understand the effect of acid concentration on reaction kinetics since acid is not only consumed in the reductive leach process, but also in the hydrogen evolution side reaction. The acid amount and concentration are directly related to process control (by solid pulp density) and economics. Acid type and concentration also affect the selection of materials of construction.

It is not recommended to state an "optimum" acid concentration for leaching because this should be determined in conjunction with all other variables, and is dictated by the particular system. The best thing that can be done is to determine the reaction dependence on hydrogen ion concentration by studying it within some reasonable range (normally 0.1–1.0 M), and use that knowledge in further assessment.

Figs. 18 and 19 summarize the effect of acid concentration on leaching kinetics for both sulfuric and hydrochloric acid solutions. As expected from the reaction written in Eq. (1), the hydrogen ion concentration has a direct effect on reaction kinetics. The extent and rate of conversion increase gradually with increasing acid concentration. However, this increase disappears after a certain limit. As was found for a set of experiments done at concentrations greater than 1.0
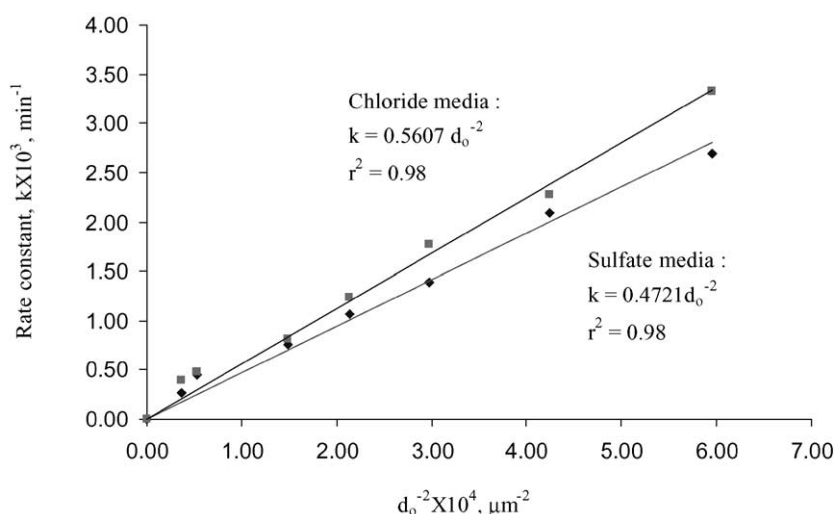

Fig. 17. Plot of parabolic leaching rate constants vs. inverse square of mean particle diameter, based on the data in Table 5.
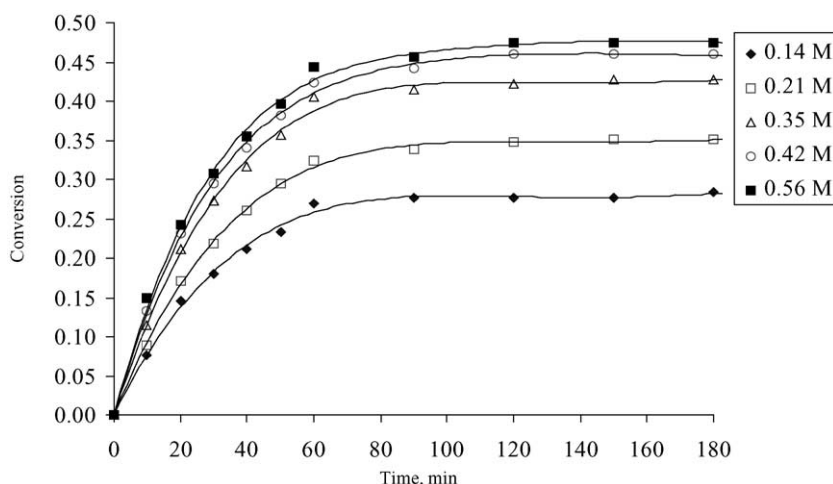
Fig. 18. Plot of conversion vs. time at various sulfuric acid concentrations (constant $CuFeS_2$ and iron additions, 25 °C).

M for sulfuric acid and 2.0 M for hydrochloric acid, the reaction rates start declining due to the severe competition from side reactions (mainly the hydrogen evolution reaction). Under such concentrations, huge gas bubbles were forming which were apparently efficient at breaking up any galvanic coupling required for the decomposition reaction to proceed.

It is clear from the indicated figures that hydrochloric acid is more efficient than sulfuric acid, with stoichiometric additions. This is attributed to the activity of the chloride ion, which will increase the

activity of the hydrogen ion. Also, the free chloride ion might play some role in affecting the leaching rates. This is due to the fact that increasing the Cl^- concentration would not only increase the hydrogen ion activity, but may also lead to a more direct participation of the chloride ion through specific adsorption or surface complexing, explaining the trend of the plot shown in Fig. 19.

From Figs. 18 and 19, it seems that reaction rates under stoichiometric additions of iron and chalcopyrite will level off at 50% conversion, which corre-
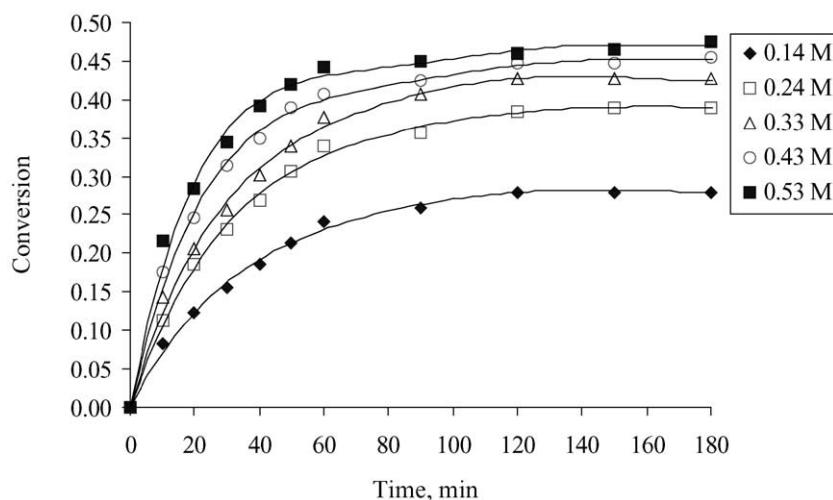

Fig. 19. Plot of conversion vs. time at various hydrochloric acid concentrations (constant $CuFeS_2$ and iron additions, 25 °C).
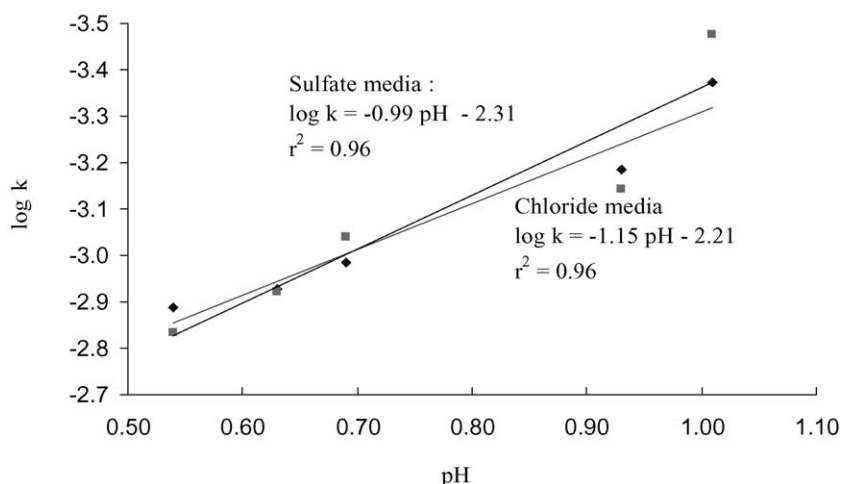
Fig. 20. Plot of log k vs. pH (constant CuFeS$_2$ and Fe additions, 25 °C). The order of parabolic leaching rate constant with respect to [H$^+$] is ~ 1. The data are based on Figs. 18 and 19.

sponds to the maximum acid concentration tested. It is concluded that best acid concentration to be used is around 0.6 M. Shirts et al. (1974) found that best conversion was obtained using sulfuric acid concentration of 0.8 M.

Fig. 20 summarizes the rate constants obtained from study of variation of acidity. In this context, the acid concentration was used instead of the activity due to the range of concentration used. The linear fitting of reaction kinetics vs. hydrogen ion concentration is a clear dependence on acid concentration, and compares well with the findings for other reductive leaching systems (Table 1). From this graph, the value of slope is approximately 1. Hence, reaction rates are first-order dependent on acid concentration [H$^+$].

By this analysis, the final forms of the kinetic models are written as:

$$1 - 3(1 - X_b)^{2/3} + 2(1 - X_b)$$
$$= \frac{k_o'}{R^2}[\text{H}^+]\exp\left(\frac{-33,900}{R'T}\right)t \tag{7}$$

$$1 - 3(1 - X_b)^{2/3} + 2(1 - X_b)$$
$$= \frac{k_o''}{R^2}[\text{H}^+]\exp\left(\frac{-22,400}{R'T}\right)t \tag{8}$$

3.6. Effect of metallic iron addition

Iron as a reactant is expected to improve the reaction kinetics and increase final conversion of chalcopyrite. Due to the importance of side reactions, it is logical to accept that more than the stoichiometric amount of iron is required for such purposes.

The direct effect of iron additions on leaching or chalcopyrite conversion can easily be seen from Figs. 21 and 22. From these figures, doubling the amount of added iron has approximately doubled the final conversion under equal additions of acid and chalcopyrite. Also, increasing the amount of iron beyond twice the stoichiometric requirements has little effect on final conversion since side reactions, such as the hydrogen evolution reaction, will more likely take place. This finding agrees well with that obtained by Shirts et al. (1974).

The effect of chalcopyrite on leaching kinetics is unlikely since the decomposition process is driven by the reductant, which will provide the required electrons, and acid, which will provide the protons, to complete Eq. (1). The significance of chalcopyrite amount arises when considering the solid pulp density. More solids imply better galvanic contact and in this case, the system is perceived to be more efficient at higher solid contents. In the ex-
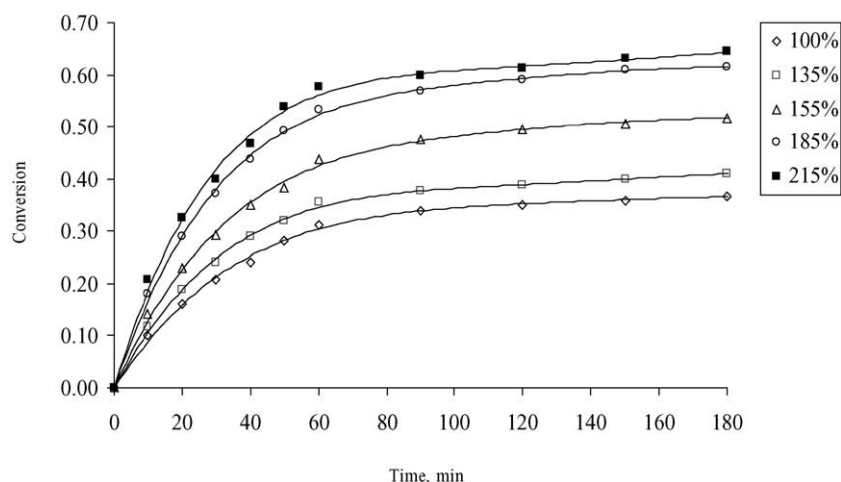
Fig. 21. Plot of conversion vs. time at various metallic iron additions (0.1 M H_2SO_4, constant $CuFeS_2$ and H_2SO_4 additions, 25 °C). The graph shows the gradual increase in reaction rates with increasing iron additions, then leveling off at values approximately twice the stoichiometric requirement.

periments performed, it was noted that the amount of iron released from chalcopyrite is almost constant, whatever the quantity of chalcopyrite added. The experiments were done at low solid content (<10%) and Figs. 23 and 24 give an idea of such an observation. The real effect of chalcopyrite is through its particle size, which was investigated previously. More discussion can be found in Abed (1999).

3.7. Schematic representation of the leaching mechanism

After this detailed analysis of leaching kinetics, it is now appropriate to develop a schematic representation of the leaching process and discuss the possible rate determining steps in the studied systems.

A schematic representation of the proposed leaching model is given in Fig. 25. In this figure, it is
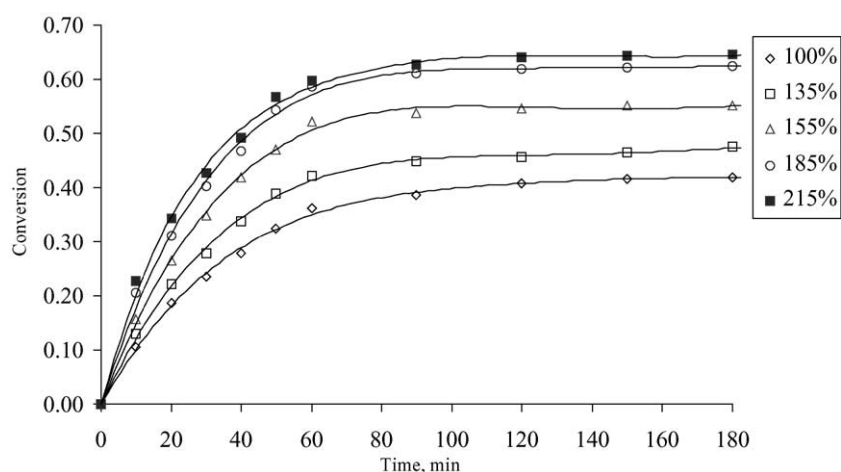

Fig. 22. Plot of conversion vs. time at various metallic iron additions (0.1 M HCl, constant $CuFeS_2$ and HCl additions, 25 °C). The graph shows the same trend as in Fig. 21.
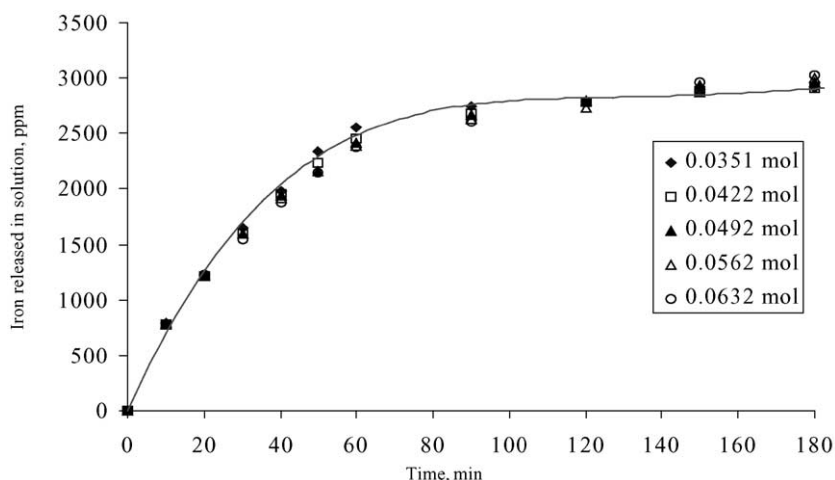
Fig. 23. Plot of iron released in solution vs. time at various chalcopyrite additions (0.1 M H_2SO_4, constant H_2SO_4 and Fe additions, 25 °C).

depicted that iron particles will form a galvanic couple with a chalcopyrite particle. Immediately, dissolution of iron occurs and its electrons are released, which will transport through the coupling or joining point to reach a suitable reaction site on the chalcopyrite particle. Simultaneously, a number of protons will diffuse from the bulk solution to this reaction site, and once these protons arrive, the reaction (Eq. (1)) will take place instantaneously. This instantaneous reaction is justified from the rapid leaching kinetics as was shown earlier. In other words, the reductive decomposition in the case of iron occurs by a combined corrosion-galvanic mechanism. For the purpose

of demonstration, one side reaction (Eq. (2)) is shown on this proposed model.

As the reaction proceeds, the new solid phase will appear as a product layer, which will cover the solid particles in the system. The exact nature of this layer was examined by SEM/EDX methods, and found to be an enriched copper phase. One analysis of the product layer gave an approximate composition in atomic percent of 61.22 at.% copper, 32.10 at.% sulfur and 6.68 at.% iron. The latter is a clear evidence for the validity of the leaching mechanism and the schematic representation of the leaching process. These results are also in conformance with the reac-
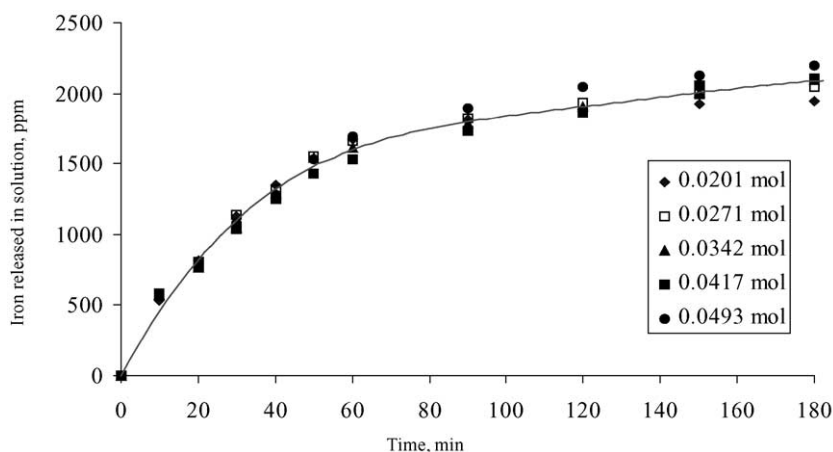

Fig. 24. Plot of iron released in solution vs. time at various chalcopyrite additions (0.1 M HCl, constant HCl and Fe additions, 25 °C).
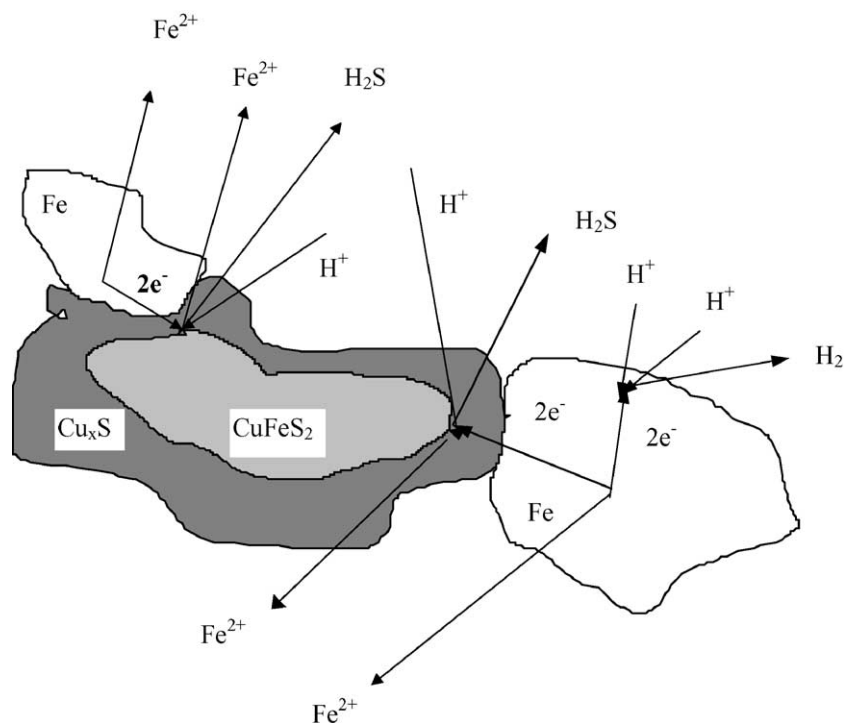
Fig. 25. Schematic representation of the galvanic conversion of chalcopyrite using metallic iron as a reductant in acidic media. The figure shows Fe–CuFeS$_2$ couples assuming iron is not surrounded by the porous product layer, and two iron particles are sharing at once in the rapid reactions. The reacted particle retains the same geometrical shape of the parent particle.

tion stoichiometry and those obtained by wet chemistry methods.

The product layer can be said to be thick and porous because reaction rates tend to level off in a short time and the observed nature of the reaction residue (a sintered or compact appearance) supports this argument. It is speculated that the product layer would cover chalcopyrite particles. Since the reaction kinetics are rapid and the chemical analysis of total iron in solution showed that it is the sum of added iron and that released from the chalcopyrite lattice, it can safely be assumed that passivation of iron particles by a product layer did not occur. This is also supported by the fact that no metallic iron was detected in the leach residue.

The thick and porous product layer surrounds the CuFeS$_2$ particle and grows inward as the particle reacts, while the solution will barely be in continuous contact with the unreacted core of chalcopyrite. The remaining chalcopyrite particle is assumed to retain the same geometrical shape as the parent particle. The product layer represents a resistance to diffusion, resulting in a diffusion overpotential (diffusion control kinetics or parabolic leaching) and a decrease in the available electrochemical driving force for the main reaction. This in turn could result in a shift to favor side reactions, such as reaction 2.

The nature of the product layer will limit the transport of different species, some of which are important to complete the reaction. It can limit the inward diffusion of protons or the outward diffusion of ferrous or sulfide ions. In the work done in this research, the only step that was proven to be rate determining, from the established leaching models in Eqs. (7) and (8), is proton diffusion. It is possible that Fe^{2+} or H$_2$S diffusion could become rate controlling under some circumstances. It is recommended that this be studied in future work.

By these points, with the previous findings of less temperature sensitivity, and large dependence on particle size, it can finally be concluded that this system is controlled by the solution transport of a species or

Chalcopyrite
concentrate

Iron

Premixing
unit

Make-up
HCl leach
solution

Recycled HCl solution to
leaching stage

H$_2$S collection
system

Sulfur product

Oxygen
and fuel

Spray roaster

Slurry system
contains :
Cu$_2$S
other sulfides
and FeCl$_2$ solution

Solid / Liquid
separation
stage

FeCl$_2$
solution

Fe$_2$O$_3$
for disposal
or tailings dam

Leaching stage

Wash water

Selected slurry recycle to adjust
SPD
contains :
Some Cu$_2$S
Other sulfides
FeCl$_2$ solution

Solid washing unit

Recycled wash
water

Cu$_2$S concentrate for
pyrometallurgical or
hydrometallurgical treatment
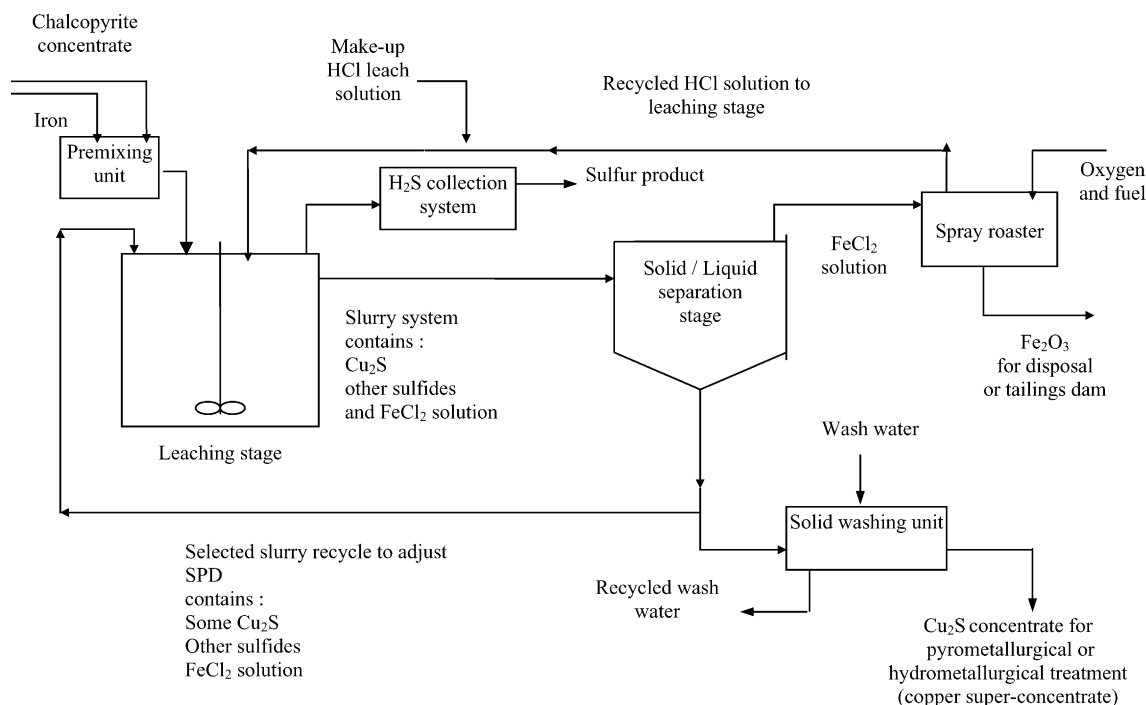(copper super-concentrate)

Fig. 26. Proposed flowsheet for processing chalcopyrite concentrates by the method of reductive leaching with metallic iron (high SPD, high recycle load of leach solution, mild conditions).

group of species through the product layer. Reductive decomposition of chalcopyrite with metallic iron is possible and this method of leaching can be utilized for the production of copper super-concentrates. Chalcocite is seemingly the new solid product (phase) of the leaching reactions.

The results of this study can now be utilized in developing a simple process flowsheet for the production of copper super-concentrates by the method of reductive decomposition. The tentative flowsheet, shown in Fig. 26, can be a good starting point for such a purpose, although more investigation is required to demonstrate its applicability and viability. The purpose here is to demonstrate the technical feasibility of the concept of reductive leaching of chalcopyrite using metallic iron. The main features of the proposed process are simplicity, recyclability and environmental compatibility with the possibility of operating at mild conditions.

As can be seen, the flowsheet comprises few unit operations and has five main steps: leaching, solid/liquid separation, washing, iron removal and sulfur

recovery. The final product is a copper-rich concentrate, which can further be treated hydrometallurgically or pyrometallurgically, depending on other factors. The flowsheet can be integrated into any existing process.

4. Concluding remarks

The schematic model in Fig. 25 is acceptable as a representation for the reductive decomposition of chalcopyrite using metallic iron. Chalcocite is the main solid product. As was confirmed from the experimental work, a transport process in the product layer controls the leaching reactions.

The shrinking core (parabolic leaching) model was selected for fitting the experimental data. Diffusion of hydrogen ions through the product layer is believed to be rate controlling. Analysis of temperature and particle size dependence confirmed the selection of the parabolic leaching models. The fitted models are shown in Eqs. (7) and (8).

Leaching kinetics are improved with increasing acid concentration and solution temperature up to a threshold value, while reaction rates are enhanced and final conversion is improved with decreasing initial particle size. Also, the leaching kinetics are much improved by increasing the iron to chalcopyrite molar ratio.

The results from the kinetic study show that maximum conversion can be obtained under the following experimental conditions:

(1) mild agitation,
(2) a temperature of 65 °C,
(3) fine particle sizes (smaller than 74 μm),
(4) an acid concentration of 0.6 M,
(5) addition of twice the stoichiometric iron requirement.

It was shown that leaching in chloride media is more efficient than that in sulfate media. A simple process flowsheet is proposed, which needs further investigation to demonstrate its viability.

Nomenclature

b	stoichiometric factor
C_{A_f}	bulk fluid concentration, or acid concentration
D_e	effective diffusivity of the fluid in the product layer. In this case, it is a function of molecular diffusivity, porosity, tortuosity, shape factor and roughness.
d_o	initial particle diameter
E_a	activation energy (kJ/mol)
$[Fe^{2+}]_{CuFeS_2}$	total iron content in chalcopyrite
$[Fe^{2+}]_{metal}$	concentration of iron due to complete metal dissolution
$[H^+]$	hydrogen ion or acid concentration
k	reaction rate constant (min^{-1}). In the case of parabolic leaching, it is parabolic leaching rate constant with the same units.
k_o	intrinsic parabolic leaching rate constant. k_o' indicates sulfate media while k_o'' indicates chloride media.
R	initial particle radius
R'	ideal gas constant, 8.314 $J\ mol^{-1}\ K^{-1}$
r^2	coefficient of determination (a statistical value)
X_b	fractional conversion with respect to solids (chalcopyrite particles)
t	time
T	recorded temperature (K)

Greek Letters

ρ_B	particle molar density (chalcopyrite)
η_{Fe}	ratio of metallic iron used in chalcopyrite reduction to total added metallic iron
Θ	ratio of total dissolved iron in solution at time t to that at the end of reaction

References

Abed, N., 1999. A Fundamental Study of the Reductive Leaching of Chalcopyrite using Metallic Iron, MASc Thesis, Metals and Materials Engineering Department, University of British Columbia, Vancouver, BC, Canada.

Chae, D.J., Wadsworth, M.E., 1979. Modeling of the Leaching of Oxide Copper Ores. Utah Univ. Press, p. 62 (Dec.).

Dasher, J., 1973. Hydrometallurgy for copper concentrates. CIM Bulletin 66 (733), 48–56 (May).

Dutrizac, J.E., MacDonald, R.J.C., 1974. Ferric ion as a leaching medium. Minerals Science and Engineering 6 (2), 59–100 (April).

Hackl, R.P., Dreisinger, D.B., Peters, E., 1987. Reverse Leaching of Chalcopyrite, pp. 181–200, In: Copper 1987—Volume 3: Hydrometallurgy and Electrometallurgy of Copper, Copper, W.C., Lagos, G.E., Ugarte, G. (Eds.), Proceedings of an International Conference, organized by the Metallurgical Society of CIM, the Chilean Institute of Mining Engineers and the University of Chile, held at the University of Chile, Santiago, Chile.

Hiskey, J.B., Wadsworth, M.E., 1975. Galvanic conversion of chalcopyrite. Metallurgical Transactions 6B, 183–190 (March).

King, J.A., Dreisinger, D.B., 1995. Autoclaving of Copper Concentrates, pp. 511–534, In: Copper 95–Cobre 95—Volume III–Electrorefining and Hydrometallurgy of Copper, Cooper, W.C., Dreisinger, D.B., Dutrizac, J., Hein, H., Ugarte, G. (Eds.), Proceedings of an International Conference sponsored, by CIM, held in Montreal, Quebec, Canada.

Levenspiel, O., 1972. Chemical Reaction Engineering, 2nd ed. Wiley, New York, NY.

O'Connor, D.J., Sexton, B.A., Smart, R.St.C. (Eds.), 1992. Surface Analysis Methods in Material Science. Springer-Verlag, Berlin, Germany.

Paynter, J.C., 1973. A review of copper hydrometallurgy. Journal of the South African Institute of Mining and Metallurgy 74 (4), 158–170 (November).

Peters, E., 1976. Direct leaching of sulfides: chemistry and applications. Metallurgical Transactions 7B, 505–517 (Dec.).

Peters, E., Swinkels, G.M., Vizsolyi, A., 1981. Copper recovery from sulfide concentrates by the UBC—cominco ferric chloride leach route. In: Kuhn, M.C. (Ed.), Process and Fundamental Considerations of Selected Hydrometallurgical Processes. SME/AIME, New York, NY, pp. 71–81.

Prasad, S., Pandey, B.D., 1998. Alternative processes for treatment of chalcopyrite. Minerals Engineering 11 (8), 763–781.

Roman, R.J., Benner, B.R., 1973. The dissolution of copper concentrates. Mineral Science and Engineering 5 (1), 3–24 (Jan.).

Shirts, M.B., Winter, J.K., Bloom, P.A., Potter, G.M., 1974. Aque-

ous Reduction of Chalcopyrite Concentrate with Metals, USBM RI 7953, US Department of the Interior, Washington, DC.

Sohn, H.-J., Wadsworth, M.E., 1980. Reduction of chalcopyrite with SO_2 in the presence of cupric ions. JOM 32 (11), 18–22 (Nov.).

Subramanian, K.N., Jennings, P.H., 1972. Review of the hydrome-tallurgy of chalcopyrite concentrates. Canadian Metallurgical Quarterly 11 (2), 387–400 (April–June).

Venkatachalam, S., 1991. Treatment of chalcopyrite concentrates by hydrometallurgical techniques. Minerals Engineering (UK) 4 (7–11), 1115–1126.